Rab27b Association with Melanosomes: Dominant Negative Mutants Disrupt Melanosomal Movement

Yanru Chen,* Preminda Samaraweera,† Tung-Tien Sun,†‡ Gert Kreibich,* and Seth J. Orlow*†

*Department of Cell Biology, †Department of Dermatology, and ‡Department of Pharmacology, New York University School of Medicine, New York, New York, U.S.A.

The movement of melanosomes from post-Golgi compartments to the periphery of melanocytes is known to be regulated by factors including myosin Va and at least one Rab protein, Rab27a. Mutations in the genes encoding either protein in the mouse result in a hypopigmented phenotype mimicking the human disease Griscelli syndrome. Rab27b and Rab27a share 72% identity and they belong to the same melanocyte/platelet subfamily of Rab proteins. Rab27a orchestrates the transport of melanosomes by recruitment of the actin motor, myosin Va, onto melanosomes. By contrast, the function of Rab27b has remained elusive. In this study, we found that Rab27b mRNA is present in melanocytes and demonstrated the intrinsic GTPase activity of Rab27b protein. We explored the function of Rab27b by overexpression of two dominant negative mutants as well as the wild-type Rab27b in melan-a melanocytes. Green-fluorescent-protein-tagged Rab27b colocalizes with the melanosome marker tyrosinase-related protein 1 and with myosin Va at the cell periphery, whereas Rab27b mutants do not decorate melanosomes, and melanosomes in these mutant transfected cells redistribute from cell periphery to the perinuclear region. Furthermore, transient overexpression of the dominant negative forms of Rab27b caused diminution in both numbers and length of dendrites of melan-a cells. Our results suggest that Rab27b may regulate the outward movement of melanosomes and the formation or maintenance of dendritic extensions in melanocytes.

Key words: GTPase/melanin/melanosome/myosin Va/Rab. J Invest Dermatol 118:930–940, 2002

Rab proteins belong to a large family of small, membrane-associated GTPases; about 60 mammalian members in this family have already been identified (Pereira-Leal and Seabra, 2000; Bock *et al*, 2001). Rab proteins may coordinate diverse cellular functions, including signal transduction, cytoskeletal organization, as well as the regulation of vesicular traffic and fusion in eukaryotic cells (Pfeffer, 1999; Zerial and McBride, 2001). These GTPases have been found to be associated with the cytoplasmic surface of distinct organelles, and with vesicles mediating transport between them. Specifically, Rab proteins are thought to be intimately involved in the process of docking and/or fusion of vesicles with their correct acceptor compartments. Regulation of specific targeting of vesicles by Rab proteins may occur at different stages of this transport process. First, Rab proteins may recruit factors involved in the biogenesis of the vesicles or they may mediate the tethering of motor molecules to the vesicle (Woodman, 1998). Rab proteins may also affect the targeting of vesicles to their appropriate destinations by interacting with Rab effector molecules that may mediate the interactions with cytoskeletal elements. For example, Rab6 mediates vesicle migration along the microtubular cytoskeleton, employing Rabkinesin-6 as the motor (Echard *et al*, 1998). Rab3 has also been shown *in vitro* to interact with α-actinin through its effector Rabphilin-3A (Arribas *et al*, 1997). These results raise the intriguing possibility that Rab proteins regulate vesicle interactions with the cytoskeleton, thereby playing an active role in membrane trafficking (Pfeffer, 1999). Rab proteins may also tether vesicles to specific components at the fusion site via Rab-interacting molecules. Rabaptin-5, EEA1, and Rabenosyn-5 are effectors associated with Rab5. Through simultaneous or sequential interactions of these docking or membrane-tethering molecules with Rab5, they orchestrate vesicle fusion (Horiuchi *et al*, 1997; Callaghan *et al*, 1999; Christoforidis *et al*, 1999; Nielsen *et al*, 2000). It was also shown that, once a vesicle has become tethered to its fusion site, Rab proteins may selectively activate the SNARE fusion machinery by removing the negative regulator Munc18 or n-Sec1 from the t-SNARE (Zhang *et al*, 2000), allowing the free t-SNARE to form the triple-helical spindle required for vesicle fusion (Lin and Scheller, 2000).

Rab proteins can be further subdivided into two families: one comprises the ''housekeeping'' Rab proteins, which are expressed in most cells and regulate basic vesicular transport common to all mammalian cells, like Rab5 regulating endosome transport (Woodman, 2000); the other includes specific Rabs, which are expressed in highly differentiated cells that carry out specialized functions. The restricted tissue distribution of certain Rab proteins may reflect specific requirements for the organization of membrane traffic in these cells. For example, the unique expression or enrichment of Rab37 in the MC-9 mast cell line and bone marrow

Manuscript received November 6, 2001; revised December 22, 2001; accepted for publication January 3, 2002.

Reprint requests to: Dr. Seth J. Orlow, Dermatology H-100, New York University School of Medicine, 560 First Avenue, New York, NY 10016, U.S.A. Email: seth.orlow@med.nyu.edu

Abbreviations: GFP, green fluorescent protein; GS, Griscelli syndrome; Lamp1, lysosome-associated membrane glycoprotein 1; MBP, maltose binding protein; TGN, *trans*-Golgi network; Tyrp1, tyrosinase-related protein 1.

cells suggests that Rab37 plays an important role in mast cell degranulation (Masuda *et al*, 2000). It appears that Rab27b may also belong to the group of Rabs that are selectively expressed in highly specialized cells.

Rab27b was originally isolated from human melanoma cells and melanocytes (Chen *et al*, 1997). Melanocytes are specialized cells in the skin and eye that express a unique elliptical membrane bounded organelle, the melanosome, which contains specific enzymes involved in melanin biosynthesis. Melanosomes contain an internal matrix upon which insoluble melanins are deposited. Based on morphologic studies, melanosomes have been described as undergoing four stages of development, namely, stage I and stage II premelanosomal compartments, partially melanized stage III melanosomes, and fully melanized stage IV melanosomes. Early models for melanosome biogenesis suggested that immature, endoplasmic-reticulum-derived organelles fuse with *trans*-Golgi network (TGN)-derived vesicles containing melanogenic components such as tyrosinase and TRP1/gp75 to form melanosomes (Quevedo *et al*, 1987; Orlow, 1998). Recent studies have suggested the alternative possibility that stage I premelanosomes are TGN-derived coated endosomes (Jimbow *et al*, 2000; Raposo *et al*, 2001). Pmel17 (gp100/silver locus protein) is the first well-characterized melanosomal protein that appears in early stage melanosomes (Kobayashi *et al*, 1994). Other melanogenic enzymes such as tyrosinase and TRP1 are added subsequently.

Melanosomes move bidirectionally along microtubules. At the cell periphery, myosin Va links melanosomes to the subcortical actin filaments in the dendritic extensions of melanocytes (Wu *et al*, 1997) from which the melanosomes are taken up by recipient cells such as neighboring keratinocytes or are inserted into nascent hair shafts.

Recent studies have shown that melanosome transport in melanocytes is highly regulated by Rab27a (Wilson *et al*, 2000; Hume *et al*, 2001; Wu *et al*, 2001). Truncation of the RAB27A gene results in the phenotype of *ashen* mice and has been implicated in Griscelli syndrome (GS, MIM 214450). GS is a rare autosomal recessive disorder that results in pigmentary dilution of the skin and hair, the presence of large clumps of pigment in hair shafts, and an accumulation of melanosomes in the perinuclear region of melanocytes. Rab27a and myosin Va were both mapped to the GS locus at chromosome 15q21 but they are 1.6 cM apart from each other (Westbroek *et al*, 2001). The phenotype of melanocytes in Rab27a-deficient *ashen* mice resembles that of melanocytes from myosin-Va-deficient *dilute* mice; they both fail to capture melanosomes in the cell periphery, resulting in the accumulation of mature melanosomes in the perinuclear region. Overexpression of the GTP-bound form but not the GDP form of Rab27a in *ashen* melanocytes rescued this defect. In addition, without functional Rab27a, myosin Va in *ashen* melanocytes does not colocalize with melanosomes (Wu *et al*, 2001). It thus seems that Rab27a recruits myosin Va to the melanosome and that myosin Va then tethers the melanosomes to subcortical actin filaments at the periphery of the cell. A direct interaction between Rab27a and myosin Va was recently shown by Hume *et al* (2001) employing coimmunoprecipitation.

Although mutations of either Rab27a or myosin Va produce the same phenotype of lightened coat color, they define two distinct subfamilies of GS. Patients with the RAB27A gene defects developed a hemophagocytic syndrome and Rab27a-deficient T cells exhibited reduced cytotoxicity and cytolytic granule exocytosis required for immune homeostasis (Menasche *et al*, 2000). The single Turkish patient with a myosin Va mutation, however, exhibited primary neurologic impairment without immune defects (Pastural *et al*, 1997), whereas Rab27a-deficient mice did not demonstrate any neurologic defect. These differences suggest that Rab27a may not be the sole partner of myosin Va.

Sequence comparison with known Rabs indicates that Rab27a and Rab27b proteins comprise a melanocyte/platelet subfamily within the Rab family (Pereira-Leal and Seabra, 2000). The expression of Rab27a and Rab27b in both melanocytes and platelets makes them candidates for involvement in mouse and human disorders characterized not only by the combination of pigment dilution and a platelet storage pool defect, but also with immunologic defects (Haddad *et al*, 2001). Despite the fact that Rab27b is the Rab protein most closely related to Rab27a, little new information emerged as it was cloned (Chen *et al*, 1997). The gene encoding human Rab27b was recently mapped to chromsome 18q21.1 (Ramalho *et al*, 2001), rather than chromosome 15 where Rab27a is located (Tolmachova *et al*, 1999). As these two highly homologous Rab proteins exhibit rather selective expression patterns, it is possible that they also possess functional overlap. On the other hand, Rab27b may also have a unique function because it cannot complement the *ashen* phenotype (Wilson *et al*, 2000). Here, we report on the tissue distribution of Rab27b in comparison with that of Rab27a by reverse transcription polymerase chain reaction (RT-PCR). The mRNA of Rab27b was present in melan-a cells and the protein was associated with melanosomes. Dominant negative forms of Rab27b do not associate with melanosomes. Overexpression of dominant-negative mutants of Rab27b not only caused redistribution of melanosomes from the cell periphery to the perinuclear region but also caused a diminution of dendrites in melan-a cells. Our results suggest that Rab27b may also play an important role in dendrite extension and in melanosome transport.

MATERIALS AND METHODS

Cell lines and antibodies Melan-a cells, cultured melanocytes from nonagouti black C57BL/6 J mice, were obtained from Dr. D. C. Bennett (St. George's Hospital, London, U.K.), and maintained as described previously (Bennett *et al* 1987). The antiserum αPEP1 raised against tyrosinase-related protein 1 (Tyrp1) was from Dr. V. J. Hearing, National Cancer Institute, Bethesda, MD (Jiménez *et al* 1991). The antiserum Dil2 against mouse myosin Va (Wu *et al*, 1997) was provided by Dr. John Hammer Jr. (National Heart, Lung and Blood Institute, Bethesda, MD). The sera were used in experiments without further purification. The rat monoclonal antibody 1D4B against murine lysosome-associated membrane glycoprotein 1 (Lamp1) (Hughes and August, 1981) was from the Developmental Studies Hybridoma Bank (University of Iowa, Iowa City, IA).

Plasmids construction Cloning procedures were performed according to standard methods (Maniatis *et al*, 1982). Enzymes and buffers were purchased from Roche (Nutley, NJ), Gibco (Gaithersburg, MD), or from New England Biolabs (Beverly, MA). The cDNA of bovine Rab27b was originally obtained by screening a bovine urothelium library, which was generated by Dr. Fang-Ming Deng in Dr. Tung-Tien Sun's laboratory (New York, NY). The coding region was cloned into pcDNA3.0 vector. Mutant forms of Rab27b, Rab27b-N133I, and Rab27b-Y29L were generated by PCR site-directed mutagenesis. Constructs were sequenced by the NYU DNA sequencing facility (Skirball Institute, New York, NY).

In order to purify Rab27b for *in vitro* GTPase assays, Rab27b and its mutant forms were cloned into the pMALC2 vector (a gift from Dr. Mindong Ren, NYU, New York, NY) between the EcoR I and Sal I sites. The resulting plasmids encode fusion proteins that contain each Rab protein or its mutants attached to the C-terminus of the maltose binding protein, abbreviated MBP-Rab27b, MBP-N133I, and MBP-Y29L. Similarly, for the expression assay, Rab27b and its mutant forms were cloned into pEEGFPC2 vector (Stratagene, La Jolla, CA) between the EcoR I and Apa I sites. The resulting plasmids encode fusion proteins that contain each Rab protein or its mutants attached to the C-terminus of the enhanced green fluorescent protein, abbreviated EGFP-Rab27b, EGFP-N133I, and EGFP-Y29L.

RNA isolation RNAs were isolated from 1–3 g of fresh tissue: urothelium scraped from bovine bladders or cultured cells from three plates (10 cm diameter) following the standard protocol (Gilman, 1997). The optical density at 260, 230, and 280 was measured to determine the amount and purity of the total RNA. Ratios of $A_{260}/A_{230} > 1.7$ and $A_{260}/A_{280} > 1.7$ were obtained. Intactness of the mRNA was inferred by intactness of 18S and 28S ribosomal RNA, as visualized on RNA agarose gels described in the next section.

RT-PCR The first-strand cDNAs for the PCR reaction were synthesized from ≈25 ng of total RNA of each tissue per reaction using

the AMV reverse transcriptase (Promega Cat. No. 3500). PCR was carried out using a PWO DNA polymerase (Roche, Nutley, NJ). Glyceraldehyde-3-phosphate dehydrogenase (GAPDH) was used as a control to determine the amount of cDNA templates and the numbers of cycles within a linear range. The optimized cycle profile for Rab27a and Rab27b was one cycle, 94°C, 3 min; 25 cycles, 94°C, 1 min; 58°C, 45 s; 72°C, 1 min; one cycle, 72°C, 7 min. Primers for Rab27a and Rab27b PCR were 27a-forward, 5′-GCCACCATGTCCGAAACTG-GATAAGCCAGC-3′; 27a-reverse, 5′-TCA AAG ATC TTA ATG TCT TCA ATG AGA C-3′; 27b-forward, ATGACCGATGGGGAC-TATGATTATCTG; 27b-reverse, 5′GGAGAAGTCAGCAGAGAAGA-AATGTGC-3′.

Site-directed mutagenesis Mutated forms of bRab27b were constructed using a point mutagenesis PCR kit from Stratagene (La Jolla, CA). PCR cycles used were 12 cycles for a single base change and 16 cycles for two or three bases change for an amino acid change: 94°C, 1 min; 55°C, 1 min; 68°C, 2 min, for each 2 kb plasmid. Primers used to generate each mutant are as follows: N133I (no GTP/GDP binding, 397–399: AAC-ATC) forward, 5′-GTA TTA ATT GGC ATC AAG GCA GAC CTG CC-3′; reverse, 5′-GG CAG GTC TGC CTT GAT GCC AAT TAA TAC-3′5′-GG CAG GTC TGC CTT GAT GCC AAT TAA TAC-3′; Y29L (85–87: TAC-TTG) forward, 5′-AAG ACA ACA TTT CTT TAT CGA TTG ACA GAC-3′; reverse, 5′-GTC TGT CAA TCG ATA AAG AAA TGT TGT CTT CCC-3′.

After the PCR, 1 μl of 5 U per μl of Dpn I restriction enzyme was added to each 50 μl PCR reaction and incubated at 37°C for 1 h to digest the circular plasmid template. 1 μl of the PCR-generated linearized plasmids was used to transform 50 μl of XL-1-blue cells (competency 10^{12} colonies per μg DNA). A single colony was inoculated on the second day for mini prep, followed by restriction enzyme digestion or sequencing to confirm the designed point mutation.

Purification of MBP fusion proteins *Escherichia coli* transformants containing MBP fusion plasmids were generated as described above. For purification, a 5 ml culture in LB containing ampicillin (50 μg per ml) was inoculated from the frozen stock and grown to saturation overnight at 37°C. The overnight cell culture was diluted into 1000 ml of medium in a 2 liter flask and grown under antibiotic selection at 37°C to an OD of 0.6 (2–4 h). IPTG was added (0.5 mM final) and the culture was grown at 37°C for an additional 3 h. After centrifuging the cell culture for 15 min, 3000 rpm at 4°C, the supernatant was decanted and the pellets were collected in a total of 10 ml of phosphate-buffered saline (PBS) containing 1 mM ethylenediamine tetraacetic acid (EDTA), 5 μg per ml aprotinin, and 1 mM phenylmethylsulfonyl fluoride, and were transferred to a 50 ml tube containing an equal volume of binding buffer pH 7.0 [10 mM $NaPO_4$ buffer pH 7.2, 0.5 M NaCl, 1 mM sodium azide, 10 mM β-mercaptoethanol, 10 mM EDTA pH 8.0, and 10 mM ethyleneglycol-bis(β-aminoethyl ether)-N,N,N′,N′-tetraacetic acid]. After sonication, 5 ml of amylase resin was washed three times with the binding buffer and added to the supernatant mixing followed by rotation for 2 h at 4°C. To elute MBP fusion proteins, the amylase resin was collected by centrifugation (1–2 min, 2000 rpm) and washed three times with binding buffer. 3 ml of 10 mM maltose in the binding buffer was added to 2 ml of resin and mixed by inverting. Usually 1–2 mg per ml of purified protein were obtained (determined by Bradford assay), and stored at 4°C for up to 1 mo. For long-term storage at −70°C, the protein concentration was increased to 4 mg per ml by adding bovine serum albumin (BSA).

GTP filter binding assay Four micrograms of purified MBP-Rab27b or its mutants were incubated at 25°C for 10 min with 1.0 μCi of [α-^{32}P]-GTP in 200 μl of a buffer containing 25 mM Tris–HCl, pH 7.5, 25 mM NaCl, 2 mM EDTA, 1 mM dithiothreitol (DTT), and 200 μg per ml BSA. $MgCl_2$ was added to a final concentration of 10 mM and the solution was then diluted with 1 ml of 25 mM Tris–HCl, pH 7.5, 25 mM NaCl, 10 mM $MgCl_2$ before passage through a nitrocellulose filter. The filter was then washed with 30 ml of the same dilution buffer and air dried, and the radioactivity retained in the filter was counted in a scintillation counter. This filter-binding assay allowed us to measure the GTP binding ability of proteins. The molar ratio of protein *versus* GTP reflects the native GTP binding capability of the GTPase because the protein retains its native conformation throughout the reaction.

GTP hydrolysis assay The determination of the GTPase activity is complicated by the fact that three different reactions affect the amount of [γ-^{32}P]-GTP bound to the Rab protein. In addition to the real enzyme activity, which hydrolyzes GTP to GDP and releases free unlabeled phosphate, there are the intrinsic GTP falling-off rate and the GTP/GDP exchange rate that cannot be ignored in the reaction system, even in the absence of GTP exchange factors. The filter-binding assay can measure the amount of GTP initially loaded, but it cannot distinguish between GTP hydrolysis *versus* exchange or off-rate. Therefore, charcoal was used to absorb proteins and nucleotides, thus enabling us to monitor the released free γ-^{32}P.

Thirty micrograms of purified Rab27b or its mutants were incubated at 25°C for 10 min with 1.0 μCi [γ-^{32}P]-GTP in 200 μl of a buffer containing 25 mM Tris–HCl, pH 7.5, 25 mM NaCl, 2 mM EDTA, 1 mM DTT, and 200 μg per ml BSA. $MgCl_2$ was added to a final concentration of 10 mM. At different time intervals, equal aliquots of the reaction mixture (≈4 μg GTPase) were withdrawn and mixed with 0.5 ml of a cold 2% wt/vol charcoal suspension in 25 mM Tris–HCl, pH 7.5, 25 mM NaCl, 10 mM $MgCl_2$. Fifty microliters of each supernatant was counted after sedimentation of the charcoal.

Sodium dodecyl sulfate polyacrylamide gel electrophoresis (SDS-PAGE) Samples were normally boiled in the sample buffer containing 0.1 M DTT or 0.1 M β-mercaptoethanol before loading. For nonreducing gels, samples were boiled in the sample buffer without adding reducing reagent. Pre-stained protein molecular weight standards were obtained from Gibco/BRL (Gaithersburg, MD). Samples were then separated on 17% acrylamide gel and stained by 0.2% Coomassie Brilliant Blue R250 (Bio-Rad, Hercules, CA).

Immunofluorescence cell staining Melan-a cells were seeded on glass coverslips in 24 well plates containing 0.5 ml medium per well or 60 mm tissue culture dishes containing 5 ml medium per dish. After 22–24 h, the cells were transfected with the plasmid containing the Rab27b coding sequence fused at its N-terminus with GFP sequence (EGFP-Rab27b). The transfection was performed using FuGene 6 transfection reagent (Roche, Indianapolis, IN) at a transfection efficiency of 10% with FuGene:DNA ratio 3:1 and DNA concentration 0.4 μg per ml culture medium as suggested by the manufacturer. 22–24 h following transfection, coverslips were rinsed with ice-cold PBS, fixed in −20°C methanol for 5 min, and air-dried. The coverslips were then blocked for 1 h in 5% goat serum in PBS, and incubated 1 h at 37°C in the primary antibody diluted in the blocking solution. They were then washed six times with 0.5% goat serum in PBS. The cells were blocked again for 30 min, and incubated for 1 h with Alexa-546-labeled secondary antibody (Molecular Probes, Eugene, OR). Coverslips were washed six times with 0.5% goat serum in PBS, rinsed with water, and mounted in ProLong Antifade (Molecular Probes). Images were acquired using the Zeiss LSM510 confocal system or with a Zeiss Axiovert 100 M microscope. Images were processed using LSM510 software and Adobe Photoshop 3.0.

Assessment of dendrite extensions in melan-a cells Melan-a melanocytes were transfected with EGFP-Rab27b or its mutant forms, whereas nontransfected cells were immunostained with the melanosome marker TRP-1. This allowed us to recognize the dendritic extensions under the fluorescence microscope as the mutant forms fill the entire cytosol. Images were systematically scanned from the left to the right of a coverslip in a meandering (S) pattern. First 18 well-stained nontransfected cells were selected for analysis. In a similar fashion, cells transfected with one of the GFP-Rab27b fusion proteins were randomly selected for assessing the changes in cell shape. The length and number of dendrites in each type of transfected melanocytes were assessed using the Zeiss LSM 510 software. Cellular extensions fitting the following criteria were counted as a dendrite: longer than 2 μm and not wider than 2 μm at the base. The histogram of **Fig 5** was generated using the CA-cricket III software.

RESULTS

Tissue distribution of Rab27a and Rab27b Because of the close sequence similarities between Rab27a and Rab27b, we first asked if the tissue expression pattern of Rab27b is similar to that of Rab27a. Although Rab27a and Rab27b share about 72% amino acid sequence similarity, RT-PCR analysis reveals that they have distinct tissue distributions. GAPDH (*panel C*) was used as control to ensure that the PCR amplification was within the linear range. Rab27a (*panel A*) and Rab27b (*panel B*) gene specific primers were designed according to the sequence of the mouse Rab27a gene (gene bank NM_023635) and a mouse Rab27b gene generated previously by 5′ and 3′ RACE reaction (gene bank AY 010898). The previously cloned Rab27b plasmid was used as the negative

control for Rab27a primers and the sequenced Rab27a PCR product was used as negative control for Rab27b primers. Rab27a primers amplified from Rab27a cDNA (*panel A, lane 2*), but not from Rab27b cDNA (*panel A, lane 1*). Rab27b primers amplified a product of expected size from Rab27b template (*panel B, lane 2*), but not from Rab27a template (*panel B, lane 1*). The annealing temperature for the PCR reaction was optimized for each pair of primers. Plasmids containing mRab27a, mRab27b, or GAPDH cDNA were used as positive controls (PC). As shown in **Fig 1**, both Rab27a and Rab27b were detected in most of the tissues tested, including bladder, kidney, melan-a cells, and spleen, but they were not detectable in muscle or liver. In certain tissues, however, distinct differences between Rab27a and Rab27b expression were observed: for example, only Rab27a mRNA was found in lung, whereas Rab27b is easily detected in whole brain.

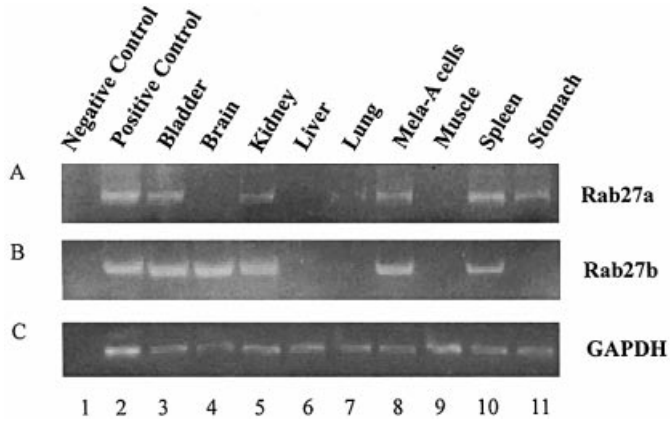

Figure 1. Tissue distribution of mouse Rab27a and mouse Rab27b as determined by RT-PCR. Total RNA was isolated from the following mouse tissues and cells: bladder, brain, kidney, liver, lung, melan-a cells, muscle, spleen, and stomach. The Rab27b plasmid was used as a negative control for the PCR amplification with Rab27a-specific primers (*A*, *lane 1*); Rab27a cDNA was used as a negative control for the PCR amplification with Rab27b-specific primers (*B*, *lane 1*). As a negative control, the GAPDH PCR reaction contained no template (*C*, *lane 1*). Rab27a cDNA confirmed by sequencing or plasmids containing mRab27b or GAPDH cDNA were used as positive controls for the gene-specific PCR amplification (*lane* 2). Specific primers were used for Rab27a (*A*), Rab27b (*panel B*), and GAPDH (*C*). Ten microliters of each PCR reaction was analyzed by agarose gel (2%) electrophoresis. Mouse Rab27b was expressed in bladder, brain, kidney, melan-a cells, and spleen. Mouse Rab27a was expressed in bladder, lung, kidney, melan-a cells, spleen, and stomach.

Point mutations alter the GTP binding capacity of Rab27b *in vitro* In order to study the function of Rab27b in melanocytes, we designed two mutated forms with point mutations chosen

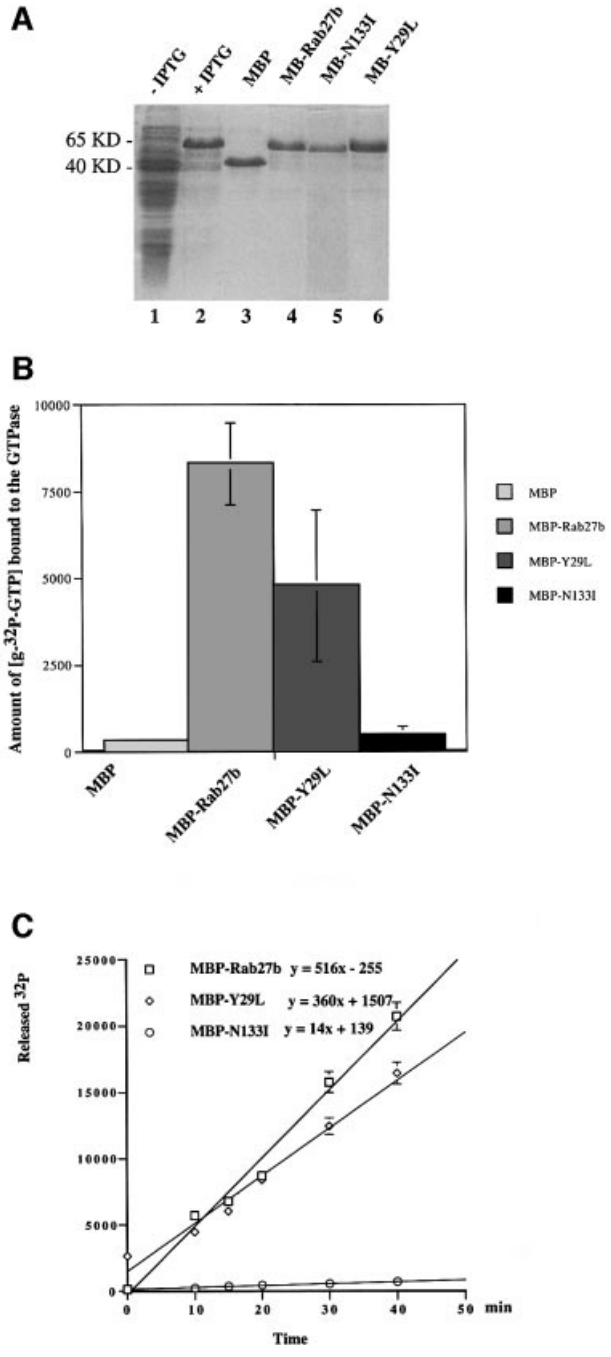

Figure 2. Purification and biochemical changes of MBP-Rab27b and its mutants. (*A*) Purification of MBP-Rab27b and its mutants from bacteria. The cDNAs encoding a fusion protein of MBP with Rab27b (MBP-Rab27b), as well as the mutant forms, were expressed in bacteria and affinity purified using an amylase resin from Bio-lab (Hercules, CA). The purified fusion protein fractions were analyzed by SDS-PAGE gel (17%), followed by Coomassie Blue staining. Cell lysate obtained before induction with isopropyl β-D thiogalactoside IPTG (*lane 1*); cell lysate obtained 3 h after induction with IPTG. As large amounts of MBP-27b protein are synthesized, 10-fold less sample was loaded for *lanes 2*, *3*, *4*, *5*, and *6*: 40 kDa purified MBP as control (*lane 3*), 65 kDa purified MBP-Rab27b (*lane 4*), purified MBP-N133I (*lane 5*), and purified MBP-Y29L (*lane 6*). (*B*) Point mutations alter GTP binding capacity of Rab27b. Four micrograms (0.16 nmol) of each MBP fusion protein of Rab27b as well as the mutant forms were immobilized on amylase resin beads and mixed with [γ-^{32}P]-GTP, where 1000 cpm corresponds to 9 pmol GTP. The stoichiometry for the wild-type Rab27b is about 0.6 mol GTP per mol GTPase. After a reaction time of 5 min, the $MgCl_2$ concentration was raised from 10 mM to 25 mM in order to prevent the dissociation of bound GTP. The enzyme-bound GTP was separated from the unbound GTP by passing the reaction through a nitrocellulose filter. The amount of radioactivity remaining on the filter represents the enzyme-bound GTP. MBP served as a negative control. The point mutation N1133I abolished the GTP binding capacity of Rab27b, whereas Y29L showed 60% binding compared with the wild-type protein. The values given in the graph are averages of three independent experiments. (*C*)Point mutations alter the GTPase activity of Rab27b. About 30 μg of the GTPases were mixed at 25°C with reaction buffer containing 10 mM $MgCl_2$. At the time points indicated, aliquots corresponding to about 4 μg GTPase were withdrawn and mixed with 600 μl of an ice-cold charcoal suspension (2%). The hydrolyzed ^{32}P, which was not absorbed by the charcoal, was measured in the supernatant after sedimentation of the charcoal-containing protein as well as free radioactive GTP. The N133I form mutant did not show any GTPase activity because it did not bind any GTP (*B*). The Y29L mutant hydrolyzes GTP at a rate similar to that of the wild-type GTPase.

according to functional studies performed on other Rab proteins. Rab27b-N133I is a dominant negative Rab mutant that does not bind GTP or GDP. The effect of the Y29L mutation on a Rab was recently described in a functional study on Cdc42 (Wu *et al*, 2000). The similar Cdc42 mutant was found to have constitutive GTPase activity in the absence of a guanine nucleotide exchange factor. In order to compare the intrinsic *in vitro* GTPase activity of these mutants with that of the wild-type Rab27b, we expressed MBP fused with Rab27b or its mutants in bacteria. The proteins were affinity purified using an amylase resin (**Fig 2*A***). MBP protein alone was used as the negative control. As shown in **Fig 2(*B*)**, MBP-Rab27b-N133I does not bind any guanine nucleotide, consistent with previous studies. On the other hand, MBP-Rab27b-Y29L binds about 60% [γ-^{32}P]-GTP compared with the wild-type Rab27b. This difference in GTP binding may be due to a lower binding capacity of the Y29L form compared to the wild-type protein. Alternatively, the binding capacity of Y29L with GTP is similar to the wild-type, but the Y29L form has a high GTPase activity due to the fact that exchange of GDP for GTP does not require specific factors or exchange proteins. The GTP binding assay that tests simply for the steady state level GTP binding did not distinguish between these two mechanisms.

The kinetics of GTPase activity of Rab27b and its mutants As may be expected from the finding that the N133I form of Rab27b does not bind GTP (**Fig 2*B***), it lacks significant GTPase activity (**Fig 2*C***). Overexpression of the N133I mutant may also affect the proper functioning of the endogenous Rab27b by depleting cells of binding proteins like GEF or GDI, thus interrupting the recycling of the wild-type Rab protein. In this way it functions as a dominant negative mutant. In the other case, the Y29L mutant hydrolyzes GTP at a rate similar to that of the wild-type Rab27b in the presence of a fixed amount of GTP (200 nM) (**Fig 2*B***). The finding that it binds about 60% of GTP compared to the wild-type Rab27b suggests that the exchange rate of GTP for GDP is slower, resulting in lower steady state binding levels.

Subcellular distribution of transiently expressed EGFP-Rab27b in melanocytes As the specific mutations in Rab27b resulted in dramatic changes in the GTPase activity of Rab27b *in vitro*, we used these mutants to determine the function of Rab27b in melanocytes. Melan-a cells are derived from inbred C57BL mice and they express the whole cycle of melanosome maturation characteristic of the differentiated state of this cell type. Melanosomes in these cells contain marker enzymes such as tyrosinase and Tyrp1 (Bennett *et al*, 1987). We took advantage of the Rab27b mutants to determine whether Rab27b functions in regulating melanosome transport, and whether the mutant forms of Rab27b could disrupt normal Rab27b function. Immunofluorescence staining was performed on melan-a cells transiently transfected with wild-type Rab27b with an enhanced GFP tag at its N-terminus (EGFP-Rab27b). As expected, the expressed EGFP-Rab27b displayed a granular distribution in melan-a cells and colocalized with melanin granules and the melanosomal marker Tyrp1, particularly in the vicinity of the plasma membrane (**Fig 3*A*–*D***). The protein also colocalized with myosin Va, a protein involved in melanosome movement (**Fig 3*E*–*H***), and to a lesser extent with the endosomal/lysosomal marker Lamp1 (**Fig 3*I*–*L***).

Transient expression of mutant forms of Rab27b result in the relocation of melanosomes from the cell periphery to the perinuclear region and diminution of both number and length of dendritic extensions To ascertain the potential biologic significance of Rab27b in melanosome translocation, we also studied the effects of two dominant negative EGFP-Rab27b mutants N133I and Y29L on melanosome distribution. When expressed in melan-a cells, both mutants resulted in diffuse cytoplasmic (both cell body and dendrites) and nuclear localization of GFP fluorescence. They caused melanosomes, identified by the presence of melanin pigment (**Fig 4*D***, ***H***, ***L***), and Tyrp1 staining (**Fig 4*A***, ***E***, ***I***) to redistribute to the perinuclear region of the cell (**Fig 4*D***, ***H***). The effect of Rab27b mutants on redistribution of melanosomes is incomplete in that only about 80% of cells exhibited concentration of melanosomes in the perinuclear area with the remainder of the cells showing a normal pattern of melanosome distribution. We attribute this to the quantity and timing of Rab27b mutant expression in transfected cells.

We noticed an apparent effect of Rab27b dominant negative mutations in dendrite formation by measuring the number and length of cellular extensions in mutant transfected cells. Taking advantage of the green florescence emitted from GFP-Rab27b constructs or the TRP1 stained control cells, we analyzed 18 cells from each category using immunofluorescence microscopy.

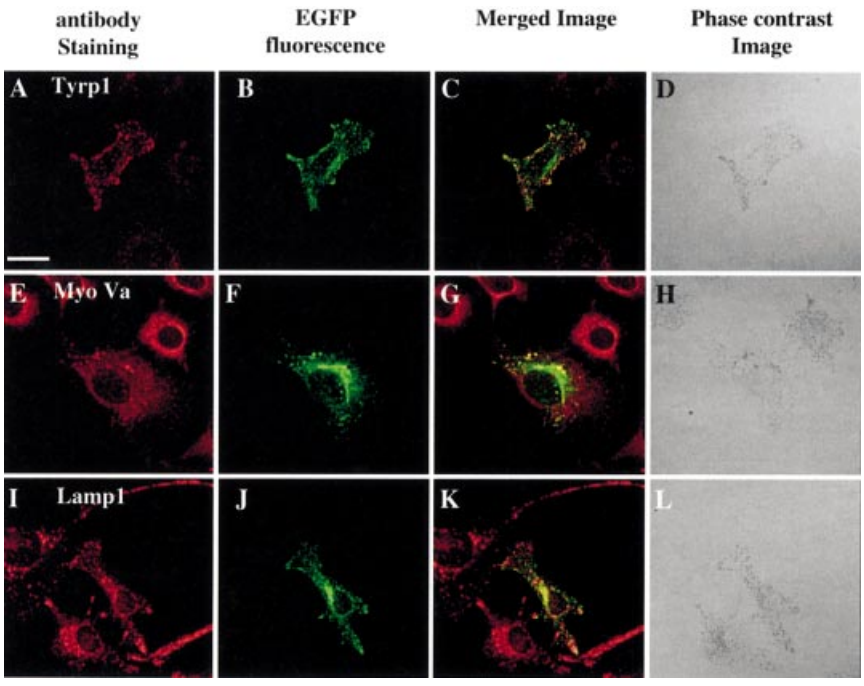

Figure 3. EGFP-Rab27b colocalizes with melanosomes but not lysosomes. Transiently expressed Rab27b protein colocalizes with melanin granules decorated by Tyrp1 and myosin Va, and to a lesser extent with lysosomes decorated by Lamp1. Melan-a cells were transfected with a plasmid encoding wild-type Rab27b protein fused at its C-terminus to GFP. 22–24 h post-transfection, all cells were fixed with methanol, and stained for Tyrp1 (*A*), myosin Va (*E*), and Lamp1 (*I*) as described in *Materials* and *Methods*. (*B*), (*F*), and (*J*) show GFP-Rab27b fluorescence of the same cell shown in the panels to the *left*. (*C*), (*G*), and (*K*) are merged images, and (*D*), (*H*), and (*L*) are phase contrast images of the cells shown in the same row. *Scale bar*: 10μm.

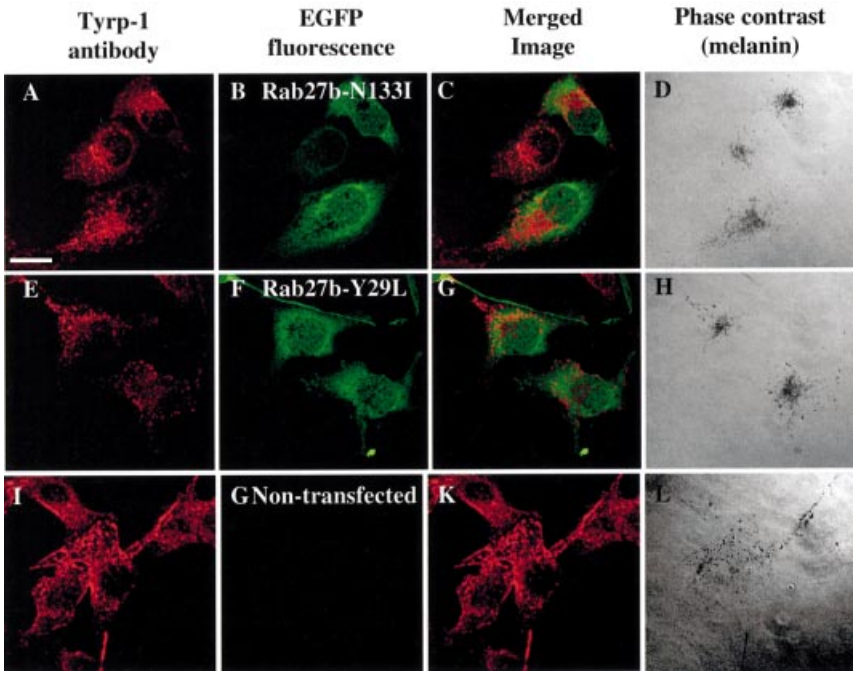

Figure 4. EGFP-Rab27b-N133I and EGFP-Rab27b-Y29L disrupt melanosome trafficking to the cell periphery. Melan-a cells were transfected with a plasmid encoding the Rab27b mutant form N133I (*A–D*) or Y29L (*E–H*) fused at its C-terminus to GFP. 24 h after transfection, all cells were fixed with methanol, and stained for Tyrp1. In untreated controls (*I*, *G*, *K*, *L*), Tyrp1 (*I*)staining and melanin distribute to the periphery of nontransfected cells. The red staining patterns (*A*)and (*E*) were obtained by immunostaining with antibody against Tyrp1. The green fluorescence corresponds to EGFP-Rab27b-N133I (*B*) and EGFP-Rab27b-Y29L (*F*). The merged images (*C*) and (*G*) showed no colocalization of Tyrp1 with the Rab27b mutant protein. Phase contrast images (*D*, *H*) demonstrate the melanin distribution in cells transfected with the Rab27b mutants. Over-expression of the dominant negative mutants, N133I and Y29L, causes melanin granules and Tyrp1 to redistribute to the perinuclear area of melan-a cells. *Scale bar*: 10μm.

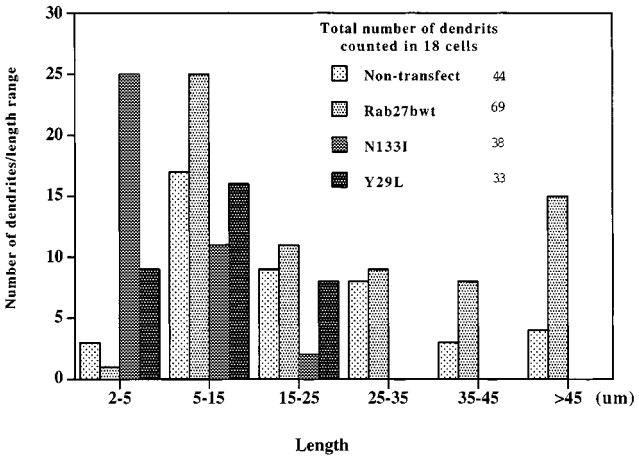

Figure 5. Overexpression of Rab27b mutants causes a diminution of dendrite number and length in melan-a cells. Transfection and staining of melan-a cells were carried out following procedures described in **Fig 4** and *Materials* and *Methods*. The length and width at the base of each dendrite was measured using the Zeiss LSM 510 software as described in *Materials* and *Methods*. Melan-a cells transfected with wild-type Rab27b have a broad distribution in the length of dendrites ranging from 2 μm to 45 μm, and a significant increase in the number of very long dendrites (>45 μm) was observed compared to the nontransfected cells. In contrast, cells transfected with dominant negative mutant constructs do not exhibit dendrites longer than 25 μm. The peak length of dendrites in cells transfected with the N133I construct was shortened to the range 2–5 μm.

Although the shapes of melan-a cells are naturally heterogeneous, we have found that the total number of dendrites in cells transfected with wild-type Rab27b (69 dendrites per 18 cells) increased 60% in comparison with nontransfected cells (44 dendrites). Furthermore, the number of very long (> 45 μm) dendritic extensions tripled in melan-a cells transfected with wild-type Rab27b compared to the nontransfected cells (**Fig 5**). In contrast, the total number of dendrites decreased to 38 in cells transfected with the dominant negative mutant N133I (≈10%) and to 33 when Y29L was expressed (≈25%). Moreover, not only did the peak length of dendrites shift to 2–5 μm in N133I and 5–15 μm in Y29L, respectively, but also no dendrites longer than 25 μm were observed in either type. To avoid missing any ''invisible'' dendrites due to the lack of melanosomes within the dendrites, a number of precautions were taken. For the wild-type Rab27b transfected or nontransfected cells we measured dendrites under phase and immunostaining with TRP1. As the GFP-Rab27b mutants are cytosolic and hence evenly distributed in both dendrites and the cell body, we measured dendrites in those cells by immunofluorescence.

DISCUSSION

Of the two Rab27 family members identified to date, only Rab27a has been assigned a cellular function, namely, melanosome trafficking. Although transient expression of EGFP-Rab27b in melanocytes showed colocalization with melanosomes (Ramalho *et al*, 2001; Westbroek *et al*, 2001), the function of Rab27b is unknown. As an initial step to understand its function we studied wild-type Rab27b and two of its dominant negative mutants. RT-PCR analysis showed that Rab27b was expressed in a number of tissues including bladder epithelium, brain, kidney, spleen, and in a cultured mouse melanocyte line, melan-a cells. Rab27a was expressed in bladder, kidney, lung, spleen, stomach, testis, and melan-a cells. The expression of Rab27b in melan-a cells was further confirmed by sequencing the amplified cDNA fragment. This finding agrees with the fact that the cDNA of Rab27b was originally cloned from melanocytes (Chen *et al*, 1997). In a recent report, however, Ramalho *et al* (2001) did not detect Rab27b in melan-a cells by RT-PCR. This discrepancy may arise from different experimental conditions employed in RT-PCR analyses, the specificity of primers, and/or the status of the cultured cells.

The current model for melanosome trafficking assumes a two-step process, namely, long-range bidirectional movement of melanosomes along microtubules and capture of the melanosomes by a random matrix of actin filaments in the cell periphery (Wu *et al*, 1998). It has been shown that defective Rab27a is one of the causes of diminished pigmentation in GS and in *ashen* mice (Menasche *et al*, 2000). Hume *et al* (2001) showed that Rab27a

regulated melanosome trafficking in melanocytes and suggested that it might function to recruit myosin Va, a molecular motor, onto melanosome membranes. Previous studies (Chen *et al*, 1997; Ramalho *et al*, 2001) as well as our analysis reported here demonstrate broad tissue distribution of Rab27a and Rab27b proteins. As overexpressed Rab27b, similar to Rab27a, is capable of associating with melanosomes, it is likely that Rab27b executes Rab27a-like functions in other tissues, presumably through myosin Va. A distinct difference between certain *dilute* mouse mutations and the *ashen* mouse is that, in the former, severe neurologic defects are observed, whereas these defects are absent in the latter. This phenotype could be due to very low expression levels of Rab27a. Alternatively, Rab27a may be expressed only in specialized areas of brain and was therefore not detected on a northern blot of whole, unfractionated brain (Chen *et al*, 1997; Ramalho *et al*, 2001). Furthermore, *dilute lethal* mice develop ataxia after 10 d of postnatal life. Abnormal tyrosine hydroxylase expression can be detected in the Purkinje cells of the cerebellum before the onset of ataxia and the extensions of the endoplasmic reticulum in the dendritic spines of these cells is missing (Dekker-Ohno *et al*, 1996; Sawada *et al*, 1999). Our data demonstrate that dominant negative forms of Rab27b cause a redistribution of melanosomes to the perinuclear area of melanocytes and a reduction both in numbers and in length of dendritic extensions. Given the 72% homology between Rab27a and Rab27b, it is possible that the dominant negative effects of overexpressed Rab27b mutants arise from other intracellular processes, perhaps indirectly through consumption of Rab27a binding proteins functioning in the Rab cycle. It is more likely, however, that Rab27b may regulate melanosome movement via myosin Va independently of Rab27a. This argument is based on the following observations. (i) Transient overexpression of Rab27b dominant negative mutants caused diminution of both numbers and length of dendrites. These phenomena were not observed in Rab27a-deficient melanocytes (Wu *et al*, 2001). (ii) The presence of Rab27b mRNA in brain can explain the neurologic defects observed in *dilute* mice. The overexpression of dominant negative mutants of Rab27b does not distinguish between a mechanism that prevents the formation of dendritic extension or one that causes existing dendrites to retract. Conceivably, Rab27b is crucial in directing the movement of melanosomes towards the cell periphery. This may be accomplished by organizing the actin filament with the help of myosin Va at the cell periphery.

We also speculate that defective Rab27b function may be the secondary cause of choroideremia (CHM), a retinal degenerative disease, classified under the broad grouping of retinitis pigment loss. The direct cause of CHM is deletions in REP-1, which is involved in the selective prenylation of Rab27a (Casey and Saeabra, 1996). Thus unprenylated Rab27a was originally thought to be the secondary cause of CHM. This explanation can be ruled out, however, because in the Rab27a-deficient mouse model *ashen* eye color was normal. This suggests that CHM may be due to a lack of prenylation of a different gene product, quite possibly Rab27b, which shares the same Rab escort protein (REP-1) with Rab27a.

Given the broad tissue distribution of Rab27a and Rab27b, it is also likely that they may function in nonmelanocytic cells to direct the trafficking of melanosome-like organelles including secretory lysosomes and related organelles (Orlow, 1998). In this study, we observed that expressed Rab27b partially colocalizes with the lysosomal protein Lamp1. Similarly, Hume *et al* (2001) observed partial colocalization of Rab27a with Lamp1 in melanocytes. Further evidence for interaction between Rab27a and lysosome-like organelles comes from GS and *ashen* mice. In both cases, the mutations in Rab27a cause defects in the function of hematopoietic cells (Wu *et al*, 1998; Menasche *et al*, 2000; Wilson *et al*, 2000). No condition involving mutations in Rab27b has been identified to date. It may be that the effect of Rab27b mutations is so subtle that it may simply have gone unnoticed or that Rab27b acts in a critical pathway in certain tissues such that any mutation that results in a defective Rab27b is lethal. Further studies on Rab27b are needed to address remaining questions pertaining to its function.

We thank Dr. Fang-Ming Deng for providing the urothelium cDNA library, Dr. Prashiela Manga for providing the melan-a RNA, and Dr. Mindong Ren and Dr. Diego Gravotta for advice on the mutant design and GTPase assay. The Zeiss LSM510 confocal microscope was purchased through NSF Major Instrumentation Award #9977430. This work was supported by NIH grant AR41880 to SJO and ACS grant DK52206 to GK.

REFERENCES

Arribas M, Regazzi R, Garcia E, Wollheim CB, De Camilli P: The stimulatory effect of rabphilin 3a on regulated exocytosis from insulin-secreting cells does not require an association–dissociation cycle with membranes mediated by Rab 3. *European J Cell Biol* 74:209–216, 1997

Bennett DC, Cooper PJ, Hart IR: A line of non-tumorigenic mouse melanocytes, syngeneic with the B16 melanoma and requiring a tumor promoter for growth. *Int J Cancer* 39:414–418, 1987

Bock JB, Matern HT, Peden AA, Scheller RH: A genomic perspective on membrane compartment organization. *Nature* 409:839–841, 2001

Callaghan J, Nixon S, Bucci C, Toh BH, Stenmark H: Direct interaction of EEA1 with Rab5b. *European J Biochem* 265:361–366, 1999

Casey P, Saeabra MC: Protein prenyltransferases. *J Biol Chem* 271:5289–5292, 1996

Chen D, Guo J, Miki T, Tachibana M, Gahl WA: Molecular cloning and characterization of Rab27a and Rab27b, novel human Rab proteins shared by melanocytes and platelets. *Biochem Mol Med* 60:27–37, 1997

Christoforidis S, McBride HM, Burgoyne RD, Zerial M: The Rab5 effector EEA1 is a core component of endosome docking. *Nature* 397:621–625, 1999

DiMaio D, Treisman R, Maniatis T: Bovine papillomavirus vector that propagates as a plasmid in both mouse and bacterial cells. *Proc Natl Acad Sci USA* 79:4030–4034, 1982

Dekker-Ohno K, Hayasaka S, Takagishi Y, *et al*: Endoplasmic reticulum is missing in dendritic spines of Purkinje cells of the ataxic mutant rat. *Brain Res* 714:226–230, 1996

Echard A, Jollivet F, Martinez O, Lacapere JJ, Rousselet A, Janoueix-Lerosey I, Goud B: Interaction of a Golgi-associated kinesin-like protein with. Rab6. *Science* 279:580–585, 1998

Gilman M: Preparation and analysis of RNA. In: Ausubel F, Brent R, Kingston R, Moore D, Seidman J, Smith J, Struhl K, eds. *Current Protocols in Molecular Biology*, New York: John Wiley & Sons, 1997:pp 414–452

Haddad EK, Wu X, Hammer JA 3rd, Henkart PA: Defective granule exocytosis in Rab27a-deficient lymphocytes from Ashen mice. [see comments].. *J Cell Biol* 152:835–842, 2001

Horiuchi H, Lippe R, McBride HM, *et al:* A novel Rab5 GDP/GTP exchange factor complexed to Rabaptin-5 links nucleotide exchange to effector recruitment and function. *Cell* 90:1149–1159, 1997

Hughes EN, August JT: Characterization of plasma membrane proteins identified by monoclonal antibodies. *J Biol Chem* 256:664–671, 1981

Hume A, Collinson L, Rapak A, Gomes A, Hopkins C, Seabra M: Rab27a regulates the peripheral distribution of melanosomes in melanocytes. *J Cell Biol* 152:F21–F24, 2001

Jimenez M, Tsukamoto K, Hearing VJ: Tyrosinases from two different loci are expressed by normal and by transformed melanocytes. *J Biol Chem* 266:1147–1156, 1991

Jimbow K, Park JS, Kato F, Hirosaki K, Toyofuku K, Hua C, Yamashita T: Assembly, target-signaling and intracellular transport of tyrosinase gene family proteins in the initial stage of melanosome biogenesis. *Pigment Cell Res* 13:222–229, 2000

Kobayashi T, Urabe K, Orlow SJ, *et al*: The Pmel 17/silver locus protein. Characterization and investigation of its melanogenic function. *J Biol Chem* 269:29198–29205, 1994

Lin RC, Scheller RH: Mechanisms of synaptic vesicle exocytosis. *Annu Rev Cell Dev Biology* 16:19–49, 2000

Masuda ES, Luo Y, Young C, et al: Rab37 is a novel mast cell specific GTPase localized to secretory granules. *FEBS Lett* 470:61–64, 2000

Menasche G, Pastural E, Feldmann J, *et al*: Mutations in RAB27A cause Griscelli syndrome associated with haemophagocytic syndrome. *Nature Genet* 25:173–176, 2000

Nielsen E, Christoforidis S, Uttenweiler-Joseph S, *et al*: Rabenosyn-5, a novel Rab5 effector, is complexed with hVPS45 and recruited to endosomes through a FYVE finger domain. *J Cell Biol* 151:601–612, 2000

Orlow SJ: The biogenesis of melanosomes. In: James E, Nordlund J, et al: eds. *The Pigmentary System: Physiology and Pathophysiology*, New York: Oxford University Press, 1998:pp 97–116

Pastural E, Barrat F, Dufourcq-Lagelouse R, *et al*: Griscelli disease maps to chromosome 15q21 and is associated with mutations in the myosinVa gene. *Nat Genet* 16:289–292, 1997

Pereira-Leal JB, Seabra MC: The mammalian Rab family of small GTPases: definition of family and subfamily sequence motifs suggests a mechanism for functional specificity in the *Ras* superfamily. *J Mol Biol* 301:1077–1087, 2000

Pfeffer SR: Transport-vesicle targeting: tethers before snares *Nature Cell Biol* 1:E17–E22, 1999

Quevedo WC, Fitzpatrick TB, Szabó G, Jimbow K: Biology of melanocytes. In: *Dermatology in General Medicine*. New York: McGraw-Hill, 1987:pp 224–251

Ramalho J, Tolmachova T, Hume A, McGuigan A, Gregory-Evans C, Huxley C,

Seabra M: Chromosomal mapping, gene structure and characterization of the human and murine RAB27B gene. *BMC Genet* 2:2–13, 2001

Raposo G, Tenzaa D, Murphyb DM, Bersonb JF, Marksb MS: Distinct protein sorting and localization to premelanosomes, melanosomes, and lysosomes in pigmented melanocytic cells. *J Cell Biol* 152:809–824, 2001

Sawada K, Komatsu S, Haga H, Oda S, Fukui Y: Abnormal expression of tyrosine hydroxylase immunoreactivity in Purkinje cells precedes the onset of ataxia in dilute-lethal mice. *Brain Res* 844:188–191, 1999

Tolmachova T, Ramalho JS, Anant JS, Schultz RA, Huxley CM, Seabra MC: Cloning, mapping and characterization of the human *RAB27A* gene. *Gene* 239:109–116, 1999

Westbroek W, Lambert J, Naeyaert J: The dilute locus and Griscelli syndrome: gateways towards a better understanding of melanosome transport. *Pigment Cell Res* 14:320–327, 2001

Wilson SM, Yip R, Swing DA, *et al*: A mutation in Rab27a causes the vesicle transport defects observed in ashen mice. *Proc Natl Acad Sci USA* 97:7933–7938, 2000

Woodman P: Vesicle transport: more work for the Rabs? *Curr Biol* 8:R199–R201, 1998

Woodman P: Biogenesis of the sorting endosome: the role of Rab5. *Traffic* 9:695–701, 2000

Wu WJ, Erickson JW, Lin R, Cerione RA: The gamma-subunit of the coatomer complex binds Cdc42 to mediate transformation. [see comments]. *Nature* 405:800–804, 2000

Wu X, Bowers B, Wei Q, Kocher B, HammerJA III: Myosin V associates with melanosomes in mouse melanocytes: evidence that myosin V is an organelle motor. *J Cell Sci* 110:847–859, 1997

Wu X, Bowers B, Rao K, Wei Q, Hammer JA: Visualization of melanosome dynamics within wild-type and dilute melanocytes suggests a paradigm for myosin V function *in vivo*, *J Cell Biol* 143:1899–1918, 1998

Wu X, Rao K, Bowers M, Copeland N, Jenkins N, Hammer JA: Rab27a enables myosin Va-dependent melanosome capture by recruiting the myosin to the organelle. *J Cell Sci* 114:1091–1100, 2001

Zerial M, McBride H: Rab proteins as membrane organizers. *Nature Rev Mol Cell Biology* 2:107–117, 2001

Zhang W, Efanov A, Yang SN, et al: Munc-18 associates with syntaxin and serves as a negative regulator of exocytosis in the pancreatic beta-cell. *J Biol Chem* 275:41521–41527, 2000